NUMERICAL INTEGRATION OF THE INCREMENTALLY NON-LINEAR, ZERO ELASTIC RANGE, BOUNDING SURFACE PLASTICITY MODEL FOR SAND

A. L. Petalas [*], Y. F. Dafalias[†]

[*] Department of Civil and Enviromental Engineering, University of California, Davis, USA
e-mail: alpetalas@ucdavis.edu

[†]Department of Civil and Enviromental Engineering, University of California, Davis, USA
and Department of Mechanics, Faculty of Applied Mathematical and Physical Sciences,
National Technical University of Athens, Greece
e-mail: jfdafalias@ucdavis.edu

Key words: constitutive equations, computational plasticity, implicit integration, bounding surface plasticity, zero elastic range

Abstract. SANISAND-Z is a recently developed plasticity model for sands with zero purely elastic range in stress space within the framework of Bounding Surface (BS) plasticity. As a consequence of zero elastic range the plastic strain increment direction, and consequently the elastic-plastic moduli fourth order tensor depends on the direction of the stress increment, rendering the model incrementally non-linear and intrinsically implicit. An iterative algorithm based on the Backward Euler method is presented to solve the non-linear system of ordinary differential equations. A non-traditional consistency condition based on the plastic multiplier is introduced as a core element of the system. A thorough analysis of the stability and accuracy of the algorithm is presented based on error estimation. The proposed integration scheme allows the use of SANISAND-Z framework in Finite Element Analysis.

1 INTRODUCTION

The idea of zero elastic range in plasticity theory was first presented by Dafalias [1] and the physical motivation was the effort to simulate the response of artificial graphite, a material which exhibits zero purely elastic range in loading and unloading [2].

In the zero elastic range bounding surface (BS) plasticity the yield surface shrinks to zero, the surface degenerates to the current stress point and the BS determines the loading direction and plastic modulus. The "image" point on the BS, at which the plastic strain rate direction is defined, is the intersection of a line along the stress increment direction with the BS. Thus, the plastic strain increment direction and consequently the fourth order elastic-plastic moduli fourth order tensor depends on the stress increment direction, rendering the model incrementally non-linear.

The numerical consequence of this type of formulation is that the model is intrinsically implicit. To solve incrementally the elasto-plastic constitutive equations, and compute the stress increment based on a given strain increment, the stress increment direction has to be specified. An iterative numerical integration scheme is proposed in this work.

2 SANISAND-Z: The model

The Sanisand-Z model developed by Dafalias and Taiebat [3] is based on the zero elastic range BS plasticity framework and the two surface formulation for sands which was presented by Manzari and Dafalias [4], Dafalias and Manzari [5] and Taiebat and Dafalias [6]. A brief discussion for the model's formulation is presented in this section, and for more details and illustrations the reader is referred to [3].

The hypoelastic moduli, K and G, are defined as functions of the isotropic stress p and the current void ratio e by:

$$G = G_0 p_{at} \frac{(2.97 - e)^2}{1 + e} \left(\frac{p}{p_{at}} \right)^{1/2} \tag{1}$$

$$K = \frac{2(1 + \nu)}{3(1 - 2\nu)} G \tag{2}$$

where p_{at} is the atmospheric pressure, ν is the poisson's ratio and G_0 a material constant.

The bounding surface (BS) and the dilatancy surface (DS) are lode angle independent and given by:

$$F^b = (\boldsymbol{r}^b : \boldsymbol{r}^b)^{1/2} - \sqrt{\frac{2}{3}} M^b = 0; \quad M^b = exp(-n^b \psi) \tag{3}$$

$$F^d = (\boldsymbol{r}^d : \boldsymbol{r}^d)^{1/2} - \sqrt{\frac{2}{3}} M^d = 0; \quad M^d = exp(-n^d \psi) \tag{4}$$

where $\boldsymbol{r} = \boldsymbol{s}/p$ is the deviatoric stress ratio tensor, n^d and n^b are material constants, and ψ is the soil state parameter [7].

The "image" point on the BS is the intersection of a line along the stress increment direction and the circular BS:

$$\boldsymbol{r}^b = \boldsymbol{r} + b\boldsymbol{\nu}; \quad b = -\boldsymbol{r} : \boldsymbol{\nu} + \left[(\boldsymbol{r} : \boldsymbol{\nu})^2 + (2/3)(M^b)^2 - \boldsymbol{r} : \boldsymbol{r} \right]^{1/2} \tag{5}$$

where $\boldsymbol{\nu}$ is a unit norm deviatoric tensor along the stress increment direction on the deviatoric plane, and b is the distance of the current stress point to the BS along the direction of the stress increment.

The loading direction is defined at the "image" point by:

$$\boldsymbol{n} = \frac{\partial F^b}{\partial \boldsymbol{r}^b} = \frac{\boldsymbol{r}^b}{|\boldsymbol{r}^b|} \tag{6}$$

Based on the loading direction the "image" point on the DS surface is given by:

$$\boldsymbol{r}^d = \sqrt{\frac{2}{3}} M^d \boldsymbol{n} \tag{7}$$

For the plastic strain rate direction $\boldsymbol{R} = \boldsymbol{R'} + (1/3)\mathrm{D}\boldsymbol{I}$ we need to determine the Dilatancy (D) and the deviatoric plastic strain rate direction ($\boldsymbol{R'}$). The dilatancy is given in Dafalias and Manzari [5] by:

$$D = A_d(\boldsymbol{r}^d - \boldsymbol{r}) : \boldsymbol{n} \tag{8}$$

Assuming a non-associative flow rule in the deviatoric plane the deviatoric plastic strain rate direction is given by:

$$\boldsymbol{R'} = B\boldsymbol{n} - C(\boldsymbol{n}^2 - \frac{1}{3}\boldsymbol{I}); \quad B = 1 + \frac{2}{3}\frac{1-c}{c}g(\theta)cos3\theta; \quad C = 3\sqrt{\frac{3}{2}}\frac{1-c}{c}g(\theta) \tag{9}$$

where θ is the lode angle and $g(\theta)$ is a non-linear function of the lode angle [5].

The plastic modulus is defined by:

$$K_p = \frac{2}{3}ph\frac{(\boldsymbol{r}^b - \boldsymbol{r}) : \boldsymbol{n}}{(\boldsymbol{r} - \boldsymbol{r}_{in}) : \boldsymbol{n}} \tag{10}$$

where $h = G_0 h_0 (1 - e)(p/p_{at})^{-0.5}$, with h_0 a material constant.

Finally, the plastic multiplier (or loading index) is given by:

$$L = \frac{1}{K_p}\boldsymbol{n} : p\dot{\boldsymbol{r}} = \frac{2G\boldsymbol{n} : \dot{\boldsymbol{e}} - K(\boldsymbol{n} : \boldsymbol{r})\dot{\epsilon}_\nu}{K_p + 2G(\boldsymbol{n} : \boldsymbol{R'}) - KD(\boldsymbol{n} : \boldsymbol{r})} \tag{11}$$

With all the plasticity formulation ingredients one can solve based on a given strain increment for the stress increment:

$$\dot{\boldsymbol{\sigma}} = 2G\dot{\boldsymbol{e}} + K\dot{\epsilon}_v\boldsymbol{I} - \langle L \rangle (2G\boldsymbol{R'} + KD\boldsymbol{I}) \tag{12}$$

3 IMPLICIT INTEGRATION

A fully implicit integration scheme is being used to integrate the rate equations outlined in the previous section. The backward Euler method together with a Damped Newton's Method is used to solve the non-linear system of ordinary differential equations. In the zero elastic range model there is no yield surface, and the enforcement of the classical consistency condition cannot be used in the iterative process.

De Borst and Heeres [8] used the definition of the plastic multiplier (L) as the replacement of the classical consistency condition for a generalized plasticity model without an explicit yield surface. Following this concept the plastic multiplier which is defined in Eq. (11) is used as the consistency parameter for the system of non-linear equations.

The stress increment tensor ($\boldsymbol{d\sigma}$) defined in Eq. 12 (notice that $\boldsymbol{d\sigma} = \dot{\boldsymbol{\sigma}}dt$) is decomposed into it's isotropic (dp) and deviatoric part ($\boldsymbol{ds}$). The independent variables of the system are defined in the following vector of unknowns:

$$U = [ds, dp, L] \tag{13}$$

The residual vector for the three unknowns is defined as follows:

$$R = [R_1, R_2, R_3] \tag{14}$$

In each iteration the algorithm solves the following linearized system:

$$\left(\frac{\partial R}{\partial U}\right)^{(k)} \delta U^{(k)} = -R^{(k)} \tag{15}$$

Finally, the updated variables are calculated by:

$$U^{(k+1)} = U^{(k)} + \lambda \delta U^{(k)} \tag{16}$$

where λ is the damping parameter which takes values smaller than 1 when the error does not decrease monotonically. The first trial guess assumes elastic stress and $L=0$.

4   NUMERICAL EXAMPLE-VERIFICATION

A numerical example is used in order to verify the numerical integration scheme. The material constants for the model are summarized in Table 1. The total strain increment which is applied and the initial stress state are given bellow:

Table 1: Sanisand-Z model parameters [3] for the numerical example

Model Constant	Symbol	Value
Elasticity	G_0	125
	ν	0.05
Critical State	M_c	1.25
	M_c	1.25
	c	0.712
	e_0	0.934
	λ	0.019
	ξ	0.7
Plastic Modulus	h_0	15
	c_h	0.
	n^b	1.25
Dilatancy	A_0	0.704
	n^d	2.1

$$\dot{\epsilon} = \begin{bmatrix} 0.01 & 0 & 0 \\ 0 & -0.006 & 0 \\ 0 & 0 & -0.006 \end{bmatrix} ; \quad \sigma^0 = \begin{bmatrix} 100 & 0 & 0 \\ 0 & 100 & 0 \\ 0 & 0 & 100 \end{bmatrix} \tag{17}$$

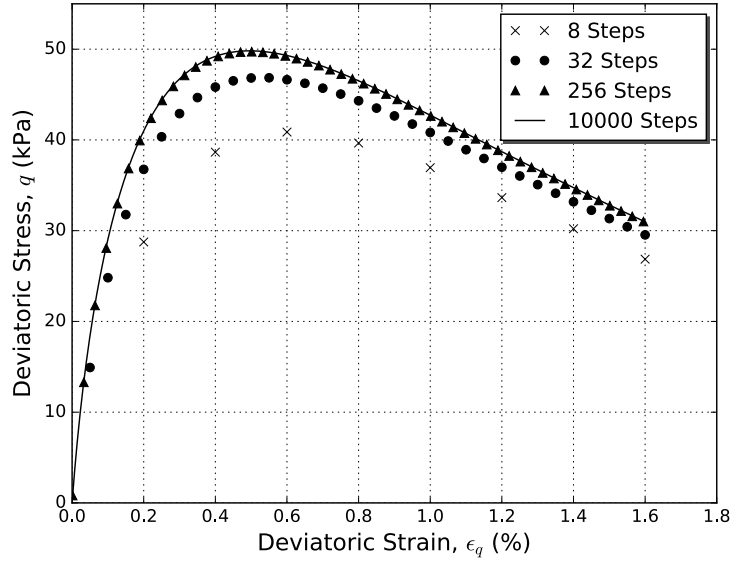A. L. Petalas [*], Y. F. Dafalias[†]

Figure 1: Stress and strain reliationship. Solution using different number of steps.

The total strain increment is applied incrementally in steps. The stress path begins from the stress state which is given by Equation (17.b) and the strain controlled test is done with the strain increment given by Equation (17.a). In Figure 1 the deviatoric stress (q) is plotted against the deviatoric strain (ϵ_q). The solution which is obtained after the application of 10000 steps is called the "accurate" solution since we lack the exact solution for this non-linear elatsto-plastic problem, and 10000 steps are enough to ensure that the solution is the converged one. We observe that the algorithm converges fast to the "accurate" solution. Moreover, even with a small number of steps (8) the integration is stable and sufficiently accurate. In Figure 2 the simulated stress path is presented. The accuracy of the algorithm is quickly improved as we move from the 8 step application towards higher number of steps.

In order to quantify the accuracy of the proposed algorithm, we compute the relative error of the computed stress for 10 simulations with different strain increment step sizes. h is the discretization parameter and the number of steps are calculated by $steps=2^h$ (h=3,4,5...12). Each discretization parameter h defines a norm of the strain increment tensor per step which is computed as follows:

$$||\dot{\boldsymbol{\epsilon}_n}|| = \frac{||\dot{\boldsymbol{\epsilon}}||}{2^h} \tag{18}$$

The relative error in a given strain level is computed as follows [9]:

$$\delta^r = \frac{\sqrt{\boldsymbol{\sigma} - \boldsymbol{\sigma}^*}}{\sqrt{\boldsymbol{\sigma}^* : \boldsymbol{\sigma}^*}} \tag{19}$$

where σ^* is the stress computed after the application of 10000 steps (the "accurate" solution). The relative error is computed for each strain level at the end of an aplied
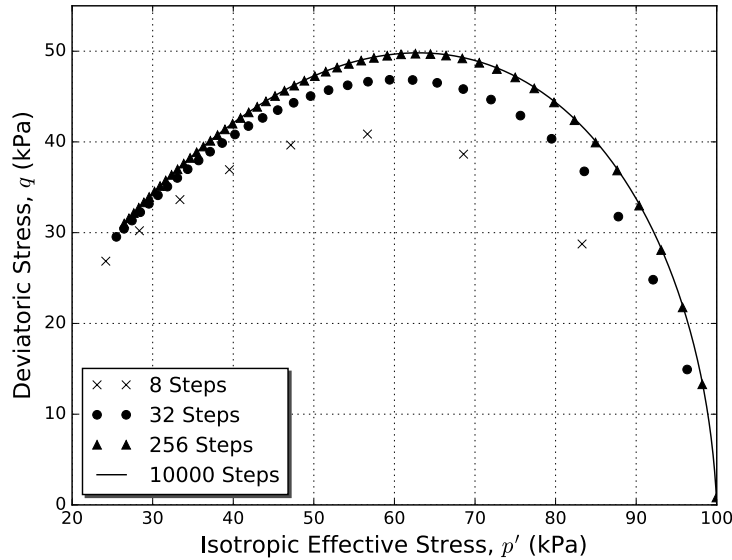
Figure 2: Stress path in the p'-q space. Solution using different number of steps.

strain increment (end of a step). We form an error vector $\boldsymbol{E}$ which has all the values of the errors computed at the end of each step. The size of this vector equals the number of steps applied for each of the simulations.

Three norms of the vector $\boldsymbol{E}$ are computed (L^1, L^2, L^∞) in order to have an error estimation for the whole numerical simulation. The three norms are defined as follows:

$$|\boldsymbol{E}|_{L1} = \sum_{r=1}^{k} |E_k| \tag{20}$$

$$|\boldsymbol{E}|_{L2} = \sqrt{\sum_{r=1}^{k} |E_k|^2} \tag{21}$$

$$|\boldsymbol{E}|_{L\infty} = \max_i |E_i| \tag{22}$$

The error estimation for the numerical test is presented in Figure 3. We observe that the error goes to zero as the strain increment per step approaches very small values for all three norms. The order of accuracy is presented in Figure 4 which depicts the rate that the error minimizes. We observe that the error minimizes linearly, when the strain increment is very small, since the order of accuracy (n) is 0.6 for the larger strain increment per step and above 1 for the smaller strain increments. This verifies that the numerical integration works accurately since the design order of accuracy of the Backward Euler method is 1 when small integration steps are being used. The Newton method shows super-linear convergence when the solution is highly non-linear and quadratic when the solution shows less non-linearity.
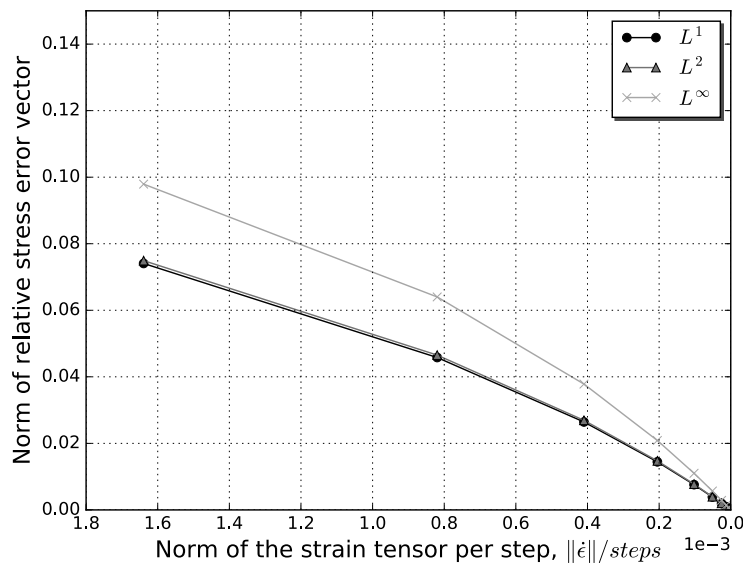
Figure 3: Relative stress error for different applied strain increments per step.

5 CONCLUSSIONS

The proposed integration scheme allow the use of the incrementally non-linear model SANISAND-Z in Finite Element Analysis. The zero elastic range bounding surface plasticity is intrinsically implicit and a iterative algorithm is needed. The system of non-linear equations solved by a Backward Euler integration scheme with Damped Newton's Method. The integration method shows 1st order accuracy for small strain increments per step. The Newton's algorithm shows super-linear convergence in the strain levels where the solution is highly non-linear, and quadratic convergence in steps when the solution is less non-linear.

6 Acknowledgments

REFERENCES

[1] Dafalias, Y.F. On cyclic and anisotropic plasticity. Ph.D. Thesis. *Department of Civil Engineering, University of California, Berkeley, CA, USA.* (1975).

[2] Dafalias, Y.F. and Popov, E. P. Cyclic loading for materials with a vanishing elastic region. *Nuclear Engineering and Design* (1977) **41**:293–302.

[3] Dafalias, Y.F. and Taiebat, M. SANISAND-Z: Zero Elastic Range Sand Plasticity Model. *Géotechnique* (2017) **66**:999–1013.
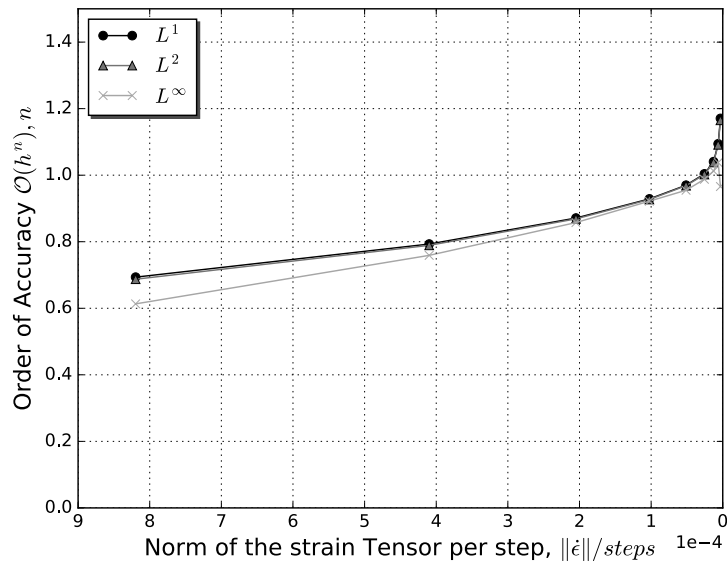
Figure 4: Order of accuracy for different applied strain increments per step.

[4] Manzari, M. T. and Dafalias, Y.F. A two-surface critical plasticity model for sand. *Géotechnique* (1997) **47**:255–272.

[5] Dafalias, Y.F. and Manzari, M. T. Simple Plasticity Sand Model Accounting for Fabric Effects *Géotechnique* (2004) **130**:622–634.

[6] Taiebat, M. and Dafalias, Y.F. SANISAND: Simple anisotropic plasticity model. *International Journal for Numerical and Analytical Methods in Geomechanics* (2008) **32**:915–948.

[7] Been, K., and Jefferies, M. G. A state parameter for sands. *Géotechnique* (1985) **35**:99–112.

[8] de Borst, R. and Heeres, O. M. A unified approach to the implicit integration of standard, non-standard and viscous plasticity models. *International Journal for Numerical and Analytical Methods in Geomechanics* (2002) **26**:1059–1070.

[9] Simo, J. C. and Hughes, T. J. R. *Computational Inelasticity.* Springer-Verlag, New York, (1998).